Synthesis, Structure and Characterizations in Solid State and Solution of Dinuclear Pentacoordinated Fe^{II} and Mn^{II} Complexes and of a Linear Tetranuclear Fe^{III} Complex Obtained with the Ligand *N*,*N*,*N*′,*N*′-Tetrakis-[(6-methyl-2-pyridyl)methyl]propane-1,3-diamine

Véronique Balland,[a] Elodie Anxolabéhère-Mallart,*[a] Frédéric Banse,*[a] Eric Rivière,[a] Sophie Bourcier,[b] Martine Nierlich,[c] and Jean-Jacques Girerd*[a]

Keywords: N ligands / Iron / Manganese / Tetranuclear complexes / Bioinorganic chemistry

Two neutral complexes $[(L_6{}^3{}4M)Fe_2Cl_4]\cdot 2H_2O\cdot 2CHCl_3$ (**1**) and $[(L_6{}^3{}4M)Mn_2Cl_4]\cdot CH_3CN$ (**2**) have been synthesized {$L_6{}^3{}4M$ = *N*,*N*,*N*′,*N*′-tetrakis[(6-methyl-2-pyridyl)methyl]propane-1,3-diamine} and their molecular structures established by X-ray crystallography. Both structures are similar, with each metal center in a trigonal-bipyramidal environment. No magnetic coupling is observed between the metal centers. UV/Vis spectra and cyclic voltammograms were recorded in CH_2Cl_2 and CH_3CN solutions. Both complexes are stable in CH_2Cl_2, whereas only **2** is stable in CH_3CN. On the contrary, **1** is in equilibrium with another Fe^{II} species in CH_3CN. When this last solution is aerated, monocrystals of the neutral linear tetranuclear complex $[(L_6{}^3{}4M)Fe_4(\mu\text{-}O)_3Cl_6]\cdot 2CH_3CN$ (**3**) can be isolated. Its structure is unusual with two Fe^{III} ions pentacoordinate and the two others tetracoordinate with only chloro ligands and oxo bridges. The magnetic properties reveal that two consecutive metal centers are strongly antiferromagnetically coupled.

Introduction

Much of the interest in the coordination chemistry of iron and manganese ions has been driven by their involvement in a number of biological systems, and in particular in the active sites of catalytic systems. Dioxygen interaction with heme- or nonheme-iron enzymes is of fundamental importance in aerobic life processes[1], including metabolism.[2,3] Whatever the system considered, interaction between dioxygen and an Fe^{II} ion leads to a superoxo adduct to Fe^{III}. In dioxygen fixation, this reaction is reversible. For substrate oxidations, reduction of the superoxo group leads to a peroxo form which evolves toward a high-valent iron−oxo entity. Often, complexes synthesized with various amine/polypyridine-, amine/polyimidazole- or polypyrazole-based ligands can reproduce the reactivity and transient peroxo motifs observed in the catalytic cycles of natural systems.[4−6]

To synthesize iron complexes, which are functional or spectroscopic models of the transient species formed during the catalytic cycle of natural systems for alkane hydroxylation, we have used a series of amine/pyridine ligands with variable length and a number of functions.[7] We report here the synthesis and structure of a dinuclear Fe^{II} complex $[(L_6{}^3{}4M)Fe_2Cl_4]\cdot 2H_2O\cdot 2CHCl_3$ (**1**) with the new hexadentate ligand *N*,*N*,*N*′,*N*′-tetrakis[(6-methyl-2-pyridyl)methyl]-propane-1,3-diamine ($L_6{}^3{}4M$; Figure 1), which upon reaction with O_2 leads to a linear tetranuclear Fe^{III} complex $[(L_6{}^3{}4M)Fe_4(\mu\text{-}O)_3Cl_6]\cdot 2CH_3CN$, (**3**). Magnetic data in the solid state, and UV/Vis and electrochemical characterizations in solution are also reported.

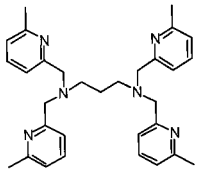

$L_6{}^3{}4M$

Figure 1. Structure of the ligand *N*,*N*,*N*′,*N*′-tetrakis[(6-methyl-2-pyridyl)methyl]propane-1,3-diamine ($L_6{}^3{}4M$)

Given the importance of Mn^{III} tetranuclear complexes in relation with the oxygen-evolving center[8,9] the previous

[a] Laboratoire de Chimie Inorganique, UMR CNRS 8613, Université Paris-Sud,
91405 Orsay, France
[b] Laboratoire des Mécanismes Réactionnels, UMR CNRS 7651, Ecole Polytechnique,
91128 Palaiseau, France
[c] DRECAM/SCM bat 125, CEA Saclay,
91191 Gif-sur-Yvette, France

result prompted us to prepare the analogous Mn complexes. Indeed, we have prepared $[(L_6{}^34M)Mn_2Cl_4]\cdot CH_3CN$ (**2**). Nevertheless, due to the higher oxidation potential for Mn^{III}/Mn^{II}, no reaction was observed with O_2. Electrochemical properties of **1** are presented and compared to those of **2**.

Results and Discussion

X-ray Crystal Structures

The structures of complexes **1** and **2** are analogous, as shown in Figures 2 and 3, respectively. The crystallographic data are reported in Table 4.

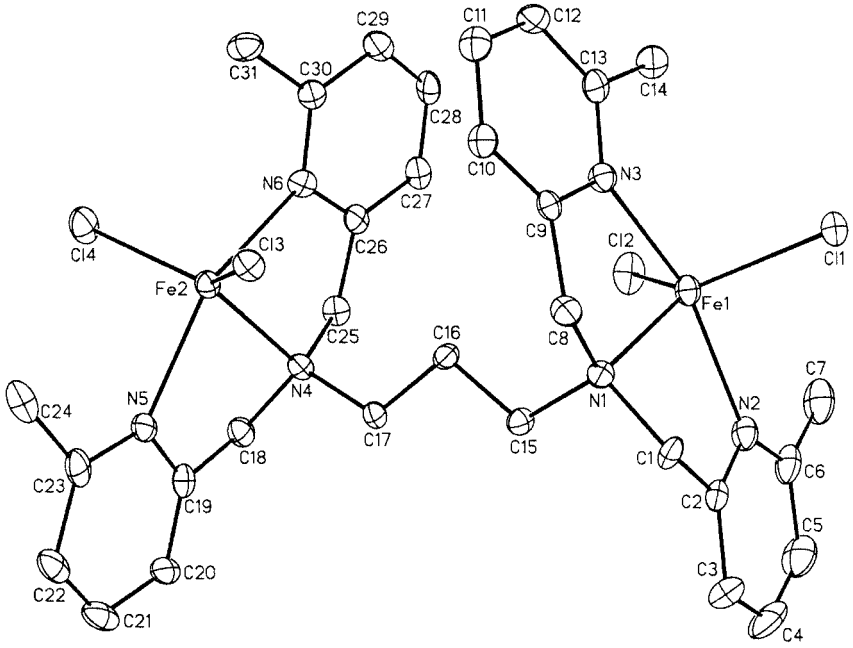

Figure 2. Crystal structure of **1** (2 H_2O and 2 $CHCl_3$ not shown)

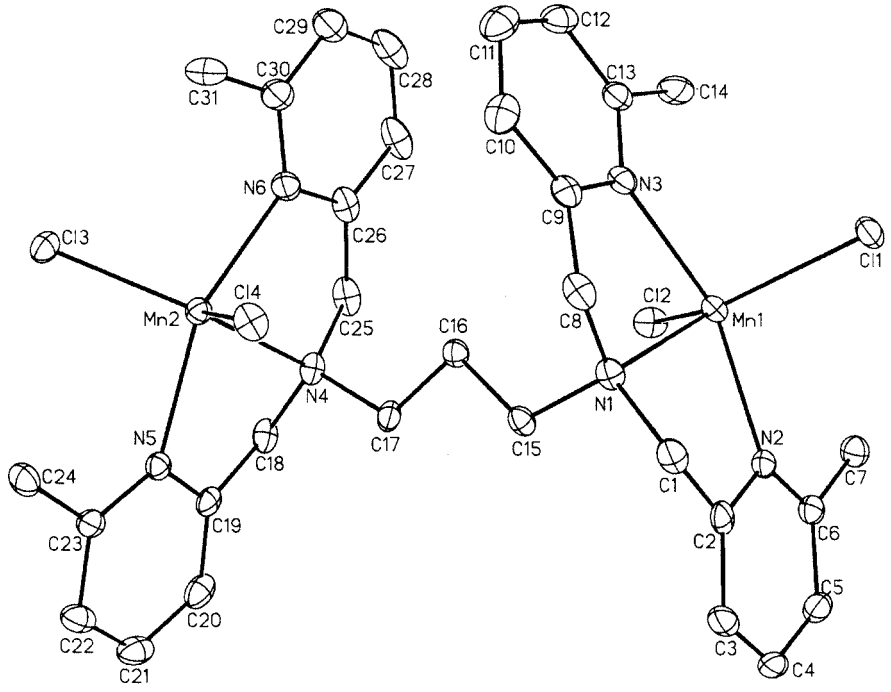

Figure 3. Crystal structure of **2** (CH_3CN not shown)

The metal/ligand ratio is 2:1 for both complexes and they exhibit two similar coordination sites. Each metal ion is surrounded by three nitrogen atoms from the ligand and two chloride ions. The geometries at the metal centers can be described as distorted trigonal bipyramids with the amino nitrogen atom, the metal center and the two chloro ligands defining the equatorial plane. Complexes containing pentacoordinate Fe^{II} ions with a similar geometry have been recently reported by Britovsek et al. with imine/pyridine ligands.[10]

The bond lengths and angles for **1** and **2** are reported in Table 1. For both complexes, the two coordination sites present small variations of the bond lengths and angles. The metal−N distances, 2.2 Å for Fe^{II} and 2.3 Å for Mn^{II}, are indicative of a high-spin state for each metal.[11−13] For complex **2** the shortest Mn−N distance occurs with the pyridine nitrogen atom, as for complexes with similar aminopyridine ligands,[14,15] which accords with a better π-acceptor character of the pyridines. The correlation between the bond lengths and the π-acceptor character of the ligand indicates minimal steric congestion at the metal center. Coordination of the ligand is therefore governed by electronic interactions. Surprisingly, this effect is not observed with the Fe^{II} complex **1**. The $Fe-N_{amino}$ bonds (ca. 2.19 Å) are shorter than the $Fe-N_{pyridine}$ ones (between 2.21 and 2.26 Å). This can be related to an enhanced steric hindrance at the metal centers in **1**. Indeed, contraction of the metal ion from Mn^{II} to Fe^{II} shortens the metal−ligand distances. However, the steric hindrance provided by the methyl groups on the pyridines lengthens the Fe−pyridine bonds.

Table 1. Selected bond lengths [Å] and angles [°] for complexes **1** and **2**

	1	**2**
M1−Cl1	2.3197(11)	2.3784(14)
M1−Cl2	2.3145(11)	2.3899(14)
M2−Cl3	2.2962(10)	2.3817(16)
M2−Cl4	2.3243(12)	2.3788(15)
M1−N1	2.188(3)	2.302(4)
M1−N2	2.253(3)	2.267(4)
M1−N3	2.217(3)	2.280(4)
M2−N4	2.192(3)	2.320(4)
M2−N5	2.256(3)	2.297(4)
M2−N6	2.230(3)	2.278(4)
Cl1−M1−Cl2	126.10(4)	123.61(6)
Cl3−M2−Cl4	128.93(4)	120.93(6)

The same conclusion is suggested by the Cl−M−Cl angles. For **1**, these are 128.93 and 126.10°, which are very similar to those of complexes with related structures.[10] Compared with **1**, the diminution of the angles observed for the Mn complex **2** (123.61 and 120.93°) is accompanied by elongation of the M−Cl bond lengths, which minimizes the repulsion between both chloride ions. Those Mn^{II}−Cl distances (around 2.38 Å) are shorter than those usually found (around 2.42 Å) for hexacoordinate Mn^{II} complexes containing at least one chloride ion. For a pseudo-square-pyramidal high-spin Mn^{II} complex containing one chloride ion, Bucher et al.[13] observed an even shorter Mn−Cl distance (2.331 Å). Therefore, the diminution of the Mn−Cl distance can be related to both the diminution of the metal coordination number and the steric hindrance around the metal center. The structure of complex **3** is represented in Figure 4.

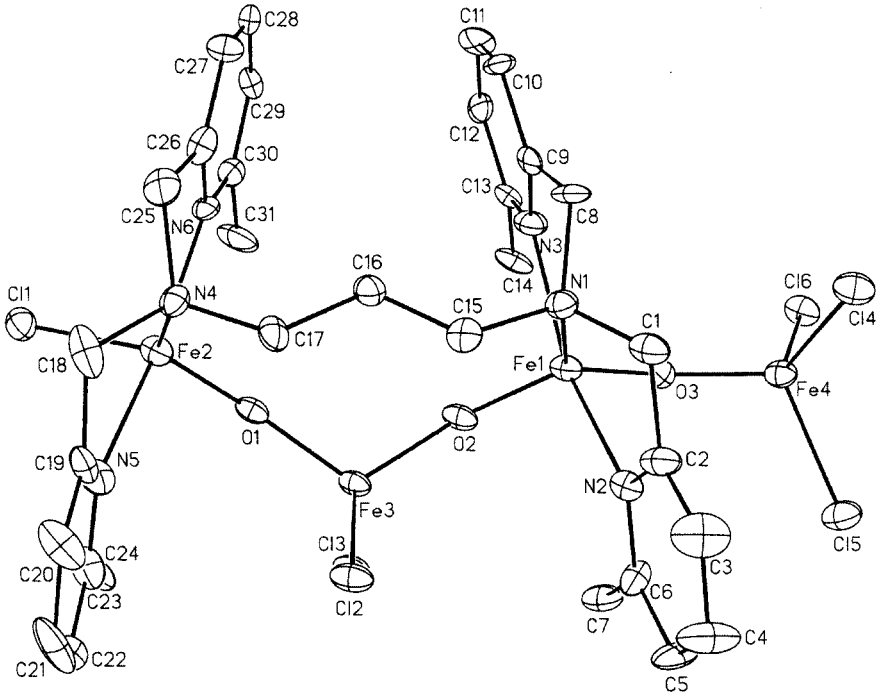

Figure 4. Crystal structure of **3** (2 CH_3CN not shown)

Table 2. Selected bond lengths [Å] and angles [°] for complex **3**

Fe1−O2	1.765(9)	Fe1−N1	2.203(11)		
Fe1−O3	1.811(9)	Fe1−N2	2.195(11)		
		Fe1−N3	2.176(10)		
Fe2−O1	1.749(9)	Fe2−N4	2.150(11)	Fe2−Cl1	2.251(4)
		Fe2−N5	2.171(11)		
		Fe2−N6	2.159(10)		
Fe3−O2	1.788(9)			Fe3−Cl2	2.260(4)
Fe3−O1	1.812(9)			Fe3−Cl3	2.246(4)
Fe4−O3	1.736(9)			Fe4−Cl4	2.256(4)
				Fe4−Cl5	2.243(4)
				Fe4−Cl6	2.248(4)
Fe1−O2−Fe3	157.3(5)				
Fe1−O3−Fe4	144.7(6)				
Fe2−O1−Fe3	151.4(5)				

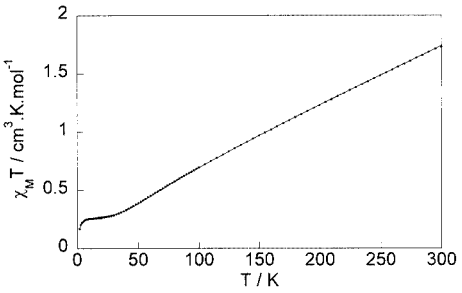

Figure 5. $\chi_M T$ vs. T for **3** (the solid line represents the best fit and the dots represent the experimental data)

The molecule is a neutral tetranuclear Fe^{III} complex, corresponding to the formula $[(L_6{}^3 4M)Fe_4(\mu\text{-}O)_3Cl_6]$. The Fe^{III} ions are in a linear configuration with three single oxo bridges. Selected bond lengths and angles are listed in Table 2.

Several reported tetranuclear Fe^{III} complexes with similar ligands[16−20] all exhibit closed structures with hexacoordinate Fe^{III} ions bridged by oxo and carboxylato groups. With the new ligand $L_6{}^3 4M$, the tetranuclear complex is linear and only two iron centers, Fe(1) and Fe(2), are coordinated to the ligand. As for **1** and **2**, the geometry at those metal centers can be considered as distorted trigonal-bipyramidal since Fe(1) and Fe(2) are surrounded by only three nitrogen atoms from the ligand and two exogeneous ligands: two oxo bridges for Fe(1) and one oxo bridge and one terminal chloride ion for Fe(2). Fe(3) and Fe(4) are not coordinated to the ligand and have tetrahedral geometries. Fe(3) is surrounded by two chloride ions and two bridging oxygen ligands, and Fe(4) by three chloride ions and one bridging oxygen ligand. The Fe(1)/Fe(4) fragment is reminiscent of unsymmetrical diiron(III) complexes.[21−25] As indicated in Table 2, all the Fe−O bond lengths are around 1.8 Å, which is typical of μ-oxo bridges for symmetrical as well as unsymmetrical units.[26] The Fe−O−Fe angles are around 150°, as observed for the other unsymmetrical (μ-oxo)diiron(III) complexes[21−24] with the exception of that reported recently by Raffard−Pons y Moll et al. (ca. 180°).[25]

An unsymmetrical structure, similar to the one of **3**, has been obtained for an $Fe^{III}-Ni^{II}$ complex with diphenylphosphate as bridging and terminal ligands.[27] Thus, the four inorganic centers are the Fe^{III}, the Ni^{II} and the P atoms. However, the structure given here for **3** is, as far as we know, the first reported tetranuclear unsymmetrical unit with only Fe^{III} ions.

Magnetic Properties

The temperature dependence of the magnetic susceptibility was measured for the three complexes in the range 300−5 K.

For complexes **1** and **2** $\chi_M T$ vs. T curves follow a Curie law, indicating no coupling between the metal ions, in agreement with the two independent coordination sites. At room temperature $\chi_M T$ is 6.7 $cm^3 \cdot K \cdot mol^{-1}$ for **1** and 8.9 $cm^3 \cdot K \cdot mol^{-1}$ for **2**. The value obtained for **1** is characteristic of two independent $S = 2$ Fe^{II} ions with $g = 2.11$. For **2**, the two Mn^{II} ions are high spin ($S = 5/2$) with a g of 2.02.

The magnetic susceptibility of the tetranuclear complex **3** as a crystalline powder material was recorded. Experimental data are represented as $\chi_M T$ vs. T in Figure 5, together with the fit.

The data were fitted to the Van Vleck formula,[28] assuming three identical oxo bridges, with full diagonalization of a $6^4 \times 6^4$ matrix. The $\chi_M T$ at 0 K differs from the zero expected and corresponds to a paramagnetic impurity, and the usual Curie−Weiss expression adapted to the high-spin Fe^{II} complex **1** was used to account for this low temperature data. The strong antiferromagnetic coupling obtained is $J = -241$ cm^{-1} and the amount of impurity is 2%. Attempts to fit the curve with three different J values have been made. The quality of the fits obtained was similar to the one reported here. Furthermore, the three J values obtained were of the same order and similar to that found when only one J was considered.

The high antiferromagnetic coupling is quite usual for single oxo-bridged unsymmetrical dinuclear Fe^{III},[21−25] and is reminiscent of the linear tetranuclear Mn^{IV} we obtained previously.[29] When the two central ions (b,c) are strongly antiferromagnetically coupled, the two terminal spins (a,d) appear to be coupled by an antiferromagnetic (AF) effective interaction. In this present case we found that if $IJ_{ab}/J_{bc}\, I << 1$ there is an effective $J_{eff} = 2.5J_{ab}{}^2/J_{bc}$. The lowest spin states are then predicted to be those of an $S_i = 5/2$ pair: $S = 0-5$. The constants obtained here led to first states of $S = 0$ ($E = 0$ cm^{-1}), $S = 1$ ($E = 114$ cm^{-1}), $S = 2$ ($E = 360$ cm^{-1}), $S = 3$ ($E = 760$ cm^{-1}). The next state is not $S = 4$ but $S = 1$ at 1014 cm^{-1}; $S = 4$ is found at $E = 1372$ cm^{-1}. The first states thus obey, qualitatively, the idea proposed, but the agreement is not quantitative since the individual J values do not obey the condition for the validity of the perturbation theory. Qualitatively, we can retain the idea that the two external spins are AF-coupled through an almost diamagnetic system, as explained by Philouze et al.[29]

EPR

The EPR spectrum of complex **2** was recorded as a frozen solution in CH_2Cl_2 at 4 K in the range 500−8000 G (Figure 6). There are no hyperfine transitions, while the broad resonances seen are typical of low-symmetry mononuclear Mn^{II} complexes,[13,30] which is consistent with the independence of the two metal centers. The main derivative line at $g = 4.2$ indicates a rhombic symmetry with E/D close to 1/3. According to this attribution, the spectrum is similar to those obtained by simulation with D between 0.2 and 0.3 cm^{-1}.[31] As far as we know, **2** is the first trigonal-bipyramidal complex with both X-ray structure and EPR characterizations.

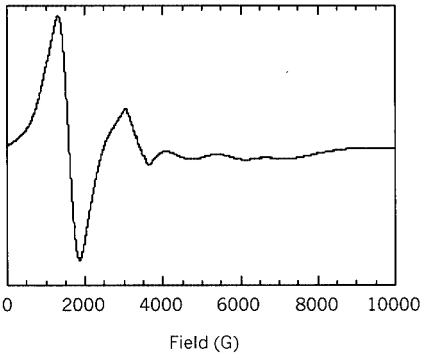

Figure 6. EPR spectra of **2** recorded in CH_2Cl_2 at 4 K at the frequency of 9.38667 GHz

No signal could be detected (at 4 K) for **3** dissolved CH_3CN. The neutral structure characterized for **3** in the solid state remains, therefore, intact in CH_3CN.

UV/Vis

UV/Vis spectra of both **1** and **2**, recorded in CH_2Cl_2, show an intense band at 268 nm that is attributed to pyridine π−π* transitions.

The Fe^{II} complex **1** shows two other bands, at 313 and 390 nm, corresponding to MLCT transitions from Fe^{II} to pyridine π* orbitals. The calculated ε values are 950 and 880 $M^{-1}\cdot cm^{-1}$, respectively. The intensity of those bands is usually around 1000 $M^{-1}\cdot cm^{-1}$ for high-spin Fe^{II} complexes.[32]

For complex **2**, no bands other than the 268 nm one are observed, except for a shoulder at 313 nm with an ε of 400 $M^{-1}\cdot cm^{-1}$.

The UV/Vis spectrum of **3** recorded in CH_3CN (Figure 7) presents three intense bands below 400 nm. The first at 262 nm is attributed to pyridine π−π* transitions with an ε of 29000 $M^{-1}\cdot cm^{-1}$. A large band with several components is observed around 335 nm (ε = 23000 $M^{-1}cm^{-1}$). In this 320−350 nm area, intense $Cl^-\rightarrow Fe^{III}$ charge-transfer bands are expected, as reported previously for dinuclear complexes with $-O-FeCl_3$ fragments,[23,25] and possibly amine-to-metal charge transfer as well.[33,34] The other intense band (381 nm, ε = 20000 $M^{-1}\cdot cm^{-1}$) may be attributed to an oxo→Fe^{III} charge-transfer transition.[35,36] The spectral features reported for μ-oxodiiron(III) complexes with aminopyridine and chloro ligands, which present an intense band around 320 nm and another at about 380 nm,[37,38] are also consistent with these assignments.

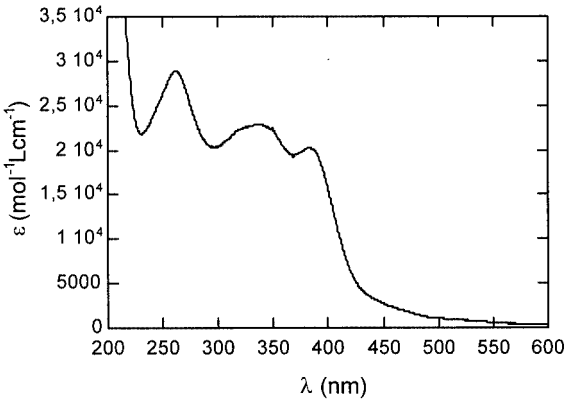

Figure 7. UV/Vis spectrum of the tetranuclear complex **3** in acetonitrile; the extinction coefficients are calculated per one molecule

Electrochemistry

The electrochemical behavior in CH_2Cl_2 of **1** (Figure 8) reveals an oxidation wave at $E_p = 0.63$ V. On the reverse scan, two waves are observed, at 0.53 and 0.04 V. Based on the peak height[39] the wave at 0.63 V is attributed to a two-electron oxidation corresponding to the simultaneous oxidation of the two Fe^{II} sites. The intensity of the cathodic wave at 0.5 V is smaller than the anodic one, thus indicating that the wave is not totally chemically reversible. Indeed, a second cathodic wave is seen on the reverse scan at a less positive potential ($E_p = 0.04$ V). The cyclic voltammogram of **1** can be compared with those reported for several complexes obtained with tetradentate aminopyridine ligand and two chloride ions. The electrochemical potentials for the Fe^{II}/Fe^{III} redox process are observed between 0 and 0.3 V.[12] The much higher potential observed here is related to the pentacoordinate geometry adopted by the iron center, which destabilizes the Fe^{III} species.

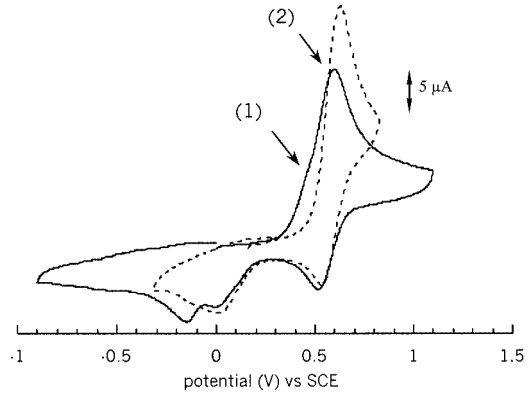

Figure 8. Cyclic voltammogram recorded in CH_2Cl_2 (- - -) and CH_3CN (———) under argon for **1**; concentration 1 mM, scan rate 100 mV s^{-1}, temperature 20 °C

The cyclic voltammogram recorded at 100 mV·s^{-1} on a CH_2Cl_2 solution of **2** (Figure 9) shows two oxidation waves, at 1.15 and 1.65 V. Reversing the potential scanning at 1.35 V allows the reversibility of the first wave to be observed ($E_{1/2}$ = 1.1 V; ΔE_p = 100 mV). The intensity of the peak indicates a two-electron process, attributed to the oxidation of the two Mn^{II} ions. The characteristic oxidation peak of the free chloride ion at 1.3 V is, notably, not observed, indicating that the two chloride ions both remain coordinated to the Mn^{II} ion and to the generated Mn^{III} center. The second oxidation wave (1.65 V) is totally irreversible, even when the scan rate is increased to 5 V s^{-1}. This second oxidation is attributed to the generation of an Mn^{IV} species − a strong oxidant that readily reacts with any trace of nucleophilic impurity in the solvent − and, therefore, no reversibility of the oxidation wave is seen under the present experimental conditions. Electrochemical data reported for Mn complexes with chloro ligands are listed in Table 3.

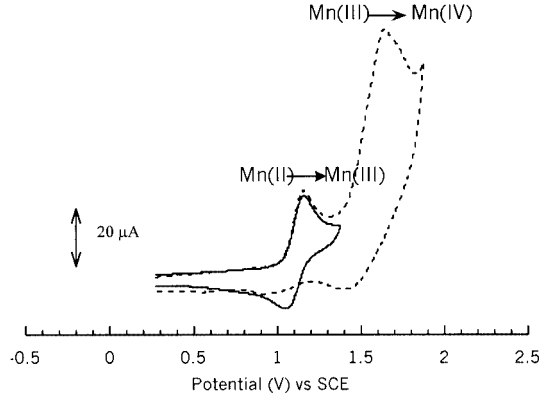

Figure 9. Cyclic voltammogram recorded in CH_2Cl_2 for **2**; concentration 1 mM, scan rate 100 mV s^{-1}, temperature 20°C

The electrochemical potential for the Mn^{II}/Mn^{III} process for **2** is much higher than those reported for mononuclear hexacoordinate Mn^{II} with two chloride ions.[40] However, it is similar to that obtained for a pentacoordinate monochloro−Mn^{II} complex for which $E_{1/2}$ = 1.14V.[13] It is surprising that the $E_{1/2}$ values are so close for both pentacoordinate complexes as the number of chloride ions coordinated is different.

In the electrogenerated $[2]^{2+}$ species the manganese ion is pentacoordinate with two chloride ions. This species was found to be more stable than the pentacoordinate monochloro−Mn^{III} complex obtained by Bucher.[13] Indeed, Bucher et al. observed a reorganization of the Mn^{III} species, leading to an hexacoordinate complex. Moreover, the pentacoordinate $[\mathbf{2}]^{2+}$ species is oxidized at a higher potential (1.65 V) than the hexacoordinate dichloro−Mn^{III} complex obtained by Hubin et al.[40] (1.33 V) and lies in the same range as the hexacoordinate monochloro−Mn^{III} complex reported by Brudenell et al. (1.56 V).[14] Complex **2** was also studied in CH_3CN. The cyclic voltammetry shows potentials identical to the one in CH_2Cl_2 solution.

Conversion of Complex 1 into Complex 3

Complex **1**, which is stable in aerated CH_2Cl_2, reacts upon O_2 exposure in CH_3CN to form complex **3**. To understand the chemical or structural modifications allowing this reactivity, complex **1** was studied in CH_3CN by cyclic voltammetry. Under argon, two anodic signals were observed, at 0.46 and 0.60 V (denoted 1 and 2 in Figure 8). The reverse scan showed three cathodic waves, at 0.5, 0 and −0.15 V. Increasing the scan rate led to the disappearance of wave 1 and the increase of wave 2 (not shown). The intensity of the resulting unique oxidation wave was identical to that observed in CH_2Cl_2 This behavior indicates that the two oxidation waves correspond to two Fe^{II} species in equilibrium. By analogy with the study in CH_2Cl_2, wave 2 is attributed to a two-electron oxidation of the neutral complex **1** and is therefore correlated to the two reduction peaks at 0.5 and 0 V. The first oxidation signal (0.46 V) is completely irreversibile. The relative intensity of waves 1 and 2 indicates that the amount of Fe^{II} species responsible for the anodic process at 0.46 V is very low in solution. Nevertheless, it is very likely that this Fe^{II} species, which forms only in CH_3CN, is responsible for the reactivity of **1** with O_2 in the same solvent. Similar behavior has been observed with a parent Fe^{II} complex,[7,25] for which the reactivity with O_2 was related to its slight instability in CH_3CN.

When the solution was open to air, the intensity of the wave at −0.15 V increased. This wave (−0.15 V) was also observed when the potential was scanned from 0.25 V towards reduction potential, thus indicating the air oxidation of the bulk solution. Concomitantly, UV/Vis spectra

Table 3. Cyclic voltammetry data for several Mn complexes; $E_{1/2}$ given vs. SCE; for irreversible waves E_P only is given

	II/III	III/IV	(II,II)/(III,III)	(III,III)/(IV,IV)	Ref.
($L_6^3$4M)Mn_2Cl_4 (**2**)			1.1	1.65 (E_P)	this work
$[Mn(L_1)Cl_2]PF_6$ [a]	0.34	1.1			[40]
$[Mn(L_2)Cl_2]PF_6$ [b]	0.16	0.93			[40]
[Mn(dmptacn)Cl]ClO_4 [c]	0.71	1.33			[14]
$[Mn_2(tmpdtnp)Cl_2](ClO_4)_2$ [d]			0.82	1.56 (E_P)	[14]
[(tmc)MnCl]BF_4 [e]	1.14	1.36			[13]

[a] L_1 = 4,11-dimethyl-1,4,8,11-tetraazabicyclo[6.6.2]hexadecane. [b] L_2 = 4,10-dimethyl-1,4,7,10-tetraazabicyclo[5.5.2]tetradecane. [c] dmptacn = 1,4-bis(2-pyridylmethyl)-1,4,7-triazacyclononane. [d] tmpdtnp = 1,3-bis[4,7-bis(2-pyridylmethyl)-1,4,7-triazacyclonon-1-yl]propane. [e] tmc = 1,4,8,11-tetramethyl-1,4,8,11-tetraazacyclotetradecanes.

were recorded on the same CH_3CN solution of **1**. The spectrum did not show any change under argon. On the contrary, two large absorption bands at 335 and 360 nm appeared when the solution was exposed to air. These new bands are tentatively attributed to the formation in CH_3CN solution of a polynuclear Fe^{III} species with Cl^- ligands and oxo bridges.[23−25] Most likely, this species is responsible for the cathodic wave at −0.15 V.

In the mass spectrum of a CH_3CN solution of **1** under air the peak seen at m/z= 836 is attributed, according to the isotopic distribution, to the $[(L_6{}^34M)Fe_3(\mu\text{-}O)_2Cl_4]^+$ cation (Figure 10). A second peak, at m/z = 621.2, is attributed to the Fe^{II} complex $[(L_6{}^34MH)FeCl_2]^+$. It is attractive to propose that the UV/Vis spectrum with absorption bands at 335 and 360 nm as well as the −0.15 V reduction wave are related to the cation $[(L_6{}^34M)Fe_3(\mu\text{-}O)_2Cl_4]^+$. The ultimate entity isolated from this CH_3CN solution was the structurally characterized tetranuclear complex $[(L_6{}^34M)Fe_4(\mu\text{-}O)_3Cl_6]$, and therefore $[(L_6{}^34M)Fe_3(\mu\text{-}O)_2Cl_4]^+$ can be considered as a precursor of the tetranuclear complex. A possible structure for $[(L_6{}^34M)Fe_3(\mu\text{-}O)_2Cl_4]^+$ is presented in Figure 11.

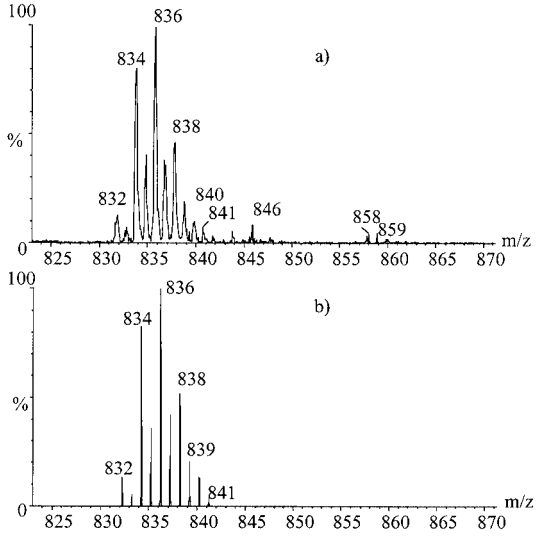

Figure 10. ESI-MS of $[(L_6{}^34M)Fe_3(\mu\text{-}O)_2Cl_4]^+$: (a) experimental spectrum; (b) calculated spectrum

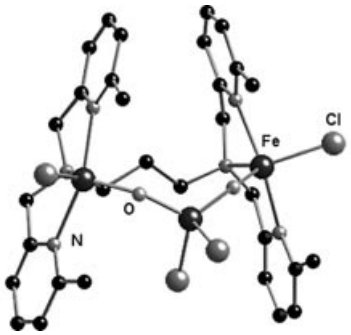

Figure 11. Possible structure for $[(L_6{}^34M)Fe_3(\mu\text{-}O)_2Cl_4]^+$

Conclusion

The neutral complexes **1** and **2** have been obtained and characterized. They present identical structures: each contains high-spin pentacoordinate metal centers in a trigonal-bipyramidal environment. The metal centers are involved in two different coordination sites and present no magnetic coupling. Both complexes are stable in CH_2Cl_2 solution and their neutral structure is retained. However, in CH_3CN, **2** is stable whereas **1** is unstable and transforms partially into a new complex species that equilibrates with **1**, as indicated by cyclic voltammogram. This latter complex is probably responsible for the reactivity of **1** with O_2 in CH_3CN, which leads to the formation of the linear tetradentate neutral complex **3**. The four metal centers are strongly antiferromagnetically coupled by single oxo bridges and exhibit different coordination sites: two are bound to the ligand and pentacoordinate whereas the two others are only tetracoordinate with chloro ligands and oxo bridges in their coordination sphere. This structure is uncommon and is, to the best of our knowledge, the first reported linear tetraferric complex.

Experimental Section

General Methods: All manipulations were carried out by using standard Schlenk techniques. Starting materials were purchased from Acros. Solvents were purchased from Merck and used without further purification.

Physical Methods: Electronic absorption spectra were recorded with a Varian Cary 5E spectrophotometer. FT-IR spectra were recorded with a Perkin−Elmer Spectrum1000 (s = sharp, i = intense, m = medium, w = weak, b = broad). Magnetic data were recorded with an MPMS5 magnetometer (Quantum Design Inc.). The calibration was made at 298 K using a palladium reference sample furnished by Quantum Design Inc. EPR spectra were recorded with an X-band Bruker ESP 300 E. Cyclic voltammograms were measured using an EGG PAR model M270 scanning potentiostat operating at a scan rate of 10−1000 mV s^{-1}. Studies were carried out under argon in acetonitrile or CH_2Cl_2 solutions using 0.2 M tetrabutylammonium perchlorate (puriss. grade, Fluka) as the supporting electrolyte, and 10^{-3} M of the complex. The working electrode was a glassy-carbon disk (0.32 cm^2) polished with 1 μm polishing powder. The reference electrode was $Ag/AgClO_4$ (+0.3 V vs. SCE), which was separated from the rest of the solution by a salt bridge containing the solvent/supporting electrolyte, with a Pt wire as an auxiliary electrode. All potentials are given vs. SCE electrode. The $E_{1/2}$ potentials are calculated as the mid-point between the anodic and the cathodic peak potentials. The mass spectra of ions formed by electrospray were acquired with a Quattro II (Micromass, Manchester, UK) triple quadrupole mass spectrometer. Typical optimized values for the source parameters were: capillary 2.5 kV, counter-electrode 0.49 kV source temperature of 80°C, RF lens 0.5 V, skimmer lens offset 0; cone voltage 20 V. Sample solutions were prepared in CH_3CN. All solutions were infused at a flow rate of 10 μL min^{-1} by a Harvard Apparatus (Southnatic, MA, USA) syringe pump. Crystallographic data were collected with a Nonius Kappa CCD area detector diffractometer[41] using graphite-monochromated Mo-K_α radiation. The lattice parameters were determined from ten images recorded with 2° -scans and later re-

Table 4. Crystallographic data for complexes **1**−**3**

	1	**2**	**3**
Empirical formula	$C_{33}H_{44}Cl_{10}Fe_2N_6O_2$	$C_{33}H_{41}Cl_4Mn_2N_7$	$C_{35}H_{44}Cl_6Fe_4N_8O_3$
Formula mass	1022.94	787.41	1060.88
Crystal size [mm]	0.20 × 0.15 × 0.05	0.20 × 0.10 × 0.10	0.10 × 0.05 × 0.01
Temperature [K]	123	123	123
Crystal system	monoclinic	monoclinic	triclinic
Space group	$P2_1/c$	$P2_1/c$	$P\bar{1}$
a [Å]	19.811(4)	15.893(3)	10.130(2)
b [Å]	8.497(2)	15.408(3)	11.743(2)
c [Å]	26.687(5)	16.796(3)	19.080(4)
α [°]	90	90	87.21(3)
β [°]	103.94(3)	116.49(3)	83.50(3)
γ [°]	90	90	85.89(3)
V [Å^3]	4360(1)	3681(1)	2247.4(8)
Z	4	4	2
μ [mm^{-1}]	1.316	1.010	1.665
F(000)	2088	1624	1080
λ (Mo-K_α)	0.71073	0.71073	0.71073
2θ range [°]	2.52, 24.71	2.71, 24.71	2.58, 24.77
$h_{min.}/h_{max.}$	0, 23	0, 18	0, 11
$k_{min.}/k_{max.}$	0, 9	0, 15	−13, 13
$l_{min.}/l_{max.}$	−31, 30	−19, 17	−19, 19
No. of measured reflections	19700	22959	13975
No. of unique reflections	7199	5811	7078
No. of refined parameters	505	415	505
$R1$ [on F^2, $I > 2\sigma(I)$]	0.0708	0.0479	0.0970
$wR2$ (on F^2)	0.1674	0.1273	0.191

fined on all data. The data were recorded at 123 K. A 180° -range was scanned with 2° steps with a crystal−detector distance fixed at 30 mm. Data were corrected for Lorentz polarization. The structures were solved by direct methods with SHELXS[42] and refined by full-matrix least squares on F^2 with anisotropic thermal parameters for all non-H atoms with SHELXL-97.[43] In complex **1**, one solvent molecule ($CHCl_3$) was disordered on two sites with 0.5 occupancy. H atoms (except H atoms of solvent molecules, CH_3Cl and H_2O in **1**, CH_3CN in **2** and **3**) were introduced at calculated positions as riding atoms with isotropic displacement parameters of 1.2 (CH, and CH_2) or 1.5 (CH_3) times that of the parent atom. Molecular plots were drawn with SHELXTL.[44] All calculations were performed with a Silicon Graphics R10000 workstation. CCDC-199949 (**1**), -199950 (**3**), -199951 (**2**) contain the supplementary crystallographic data for this paper. These data can be obtained free of charge at www.ccdc.cam.ac.uk/conts/retrieving.html [or from the Cambridge Crystallographic Data Centre, 12 Union Road, Cambridge CB2 1EZ, UK; Fax: (internat.) + 44-1223/336-033; E-mail: deposit@ccdc.cam.ac.uk].

Synthesis of $L_6^3$4M: *N*,*N*,*N*′,*N*′-Tetrakis[(6-methyl-2-pyridyl)methyl]propane-1,3-diamine. The ligand was synthesized as *N*,*N*,*N*′,*N*′-tetrakis(2-pyridylmethyl)ethane-1,2-diamine[45] using 2-(chloromethyl)-6-methylpyridine hydrochloride (8 g) and propane-1,3-diamine (835 μL) as starting materials. The product was recrystallized from cyclohexane and obtained as a white powder (4.35 g).

Synthesis of $[(L_6^3$4M)$Fe_2Cl_4]\cdot 2H_2O\cdot 2CHCl_3$ (1): 1 equiv. of ligand (100 mg) in THF (2 mL) was added to a solution of 2 equiv. of $FeCl_2\cdot 2H_2O$ (66 mg) in THF (3 mL) under argon. The mixture was then stirred at room temperature for 30 min and concentrated. After removal of most of the solvent, a yellow solid precipitated, which was filtered off (80 mg, 53% yield). $C_{31}H_{38}Cl_4Fe_2N_6\cdot H_2O$ (766.21): calcd. C 48.60, H 5.26, N 10.97; found C 48.66, H, 5.22, N 10.33. FT-IR: $\tilde{\nu}$ = 1605 (s, i), 1577 (s, m), 1458 (s, i), 1043 (s, w), 1010 (s, m), 841 (s, w), 782 (s, m) cm^{-1}. Crystals of **1** were obtained by slow diffusion of *tert*-butyl methyl ether into a solution of the powder dissolved in $CHCl_3$.

Synthesis of $[(L_6^3$4M)$Mn_2Cl_4]\cdot 2CH_3CN$ (2): 1 equiv. of ligand (50 mg) in THF (2 mL) was added to a solution of 2 equiv. of $MnCl_2\cdot 4H_2O$ (40 mg) in THF (4 mL). The mixture was then stirred at room temperature for 30 min, and the resultant white precipitate was filtered off and collected (56 mg, 74% yield). $C_{31}H_{38}Cl_4Mn_2N_6$ (746.4): calcd. C 49.88, H 5.13, N 11.26; found C 49.19, H, 5.17, N 11.97. FT-IR: $\tilde{\nu}$ = 1607 (s, i), 1578 (s, i), 1454 (s, i), 1043 (s, w), 1010 (s, mi), 860 (s, m), 781 (b, m), 300 (b, m) cm^{-1}. The white powder was dissolved in CH_3CN and crystals of **2** were obtained by slow diffusion of *tert*-butyl methyl ether into the solution. All characterizations of complex **2** were performed with crystals.

Synthesis of $[(L_6^3$4M)$Fe_4(\mu\text{-}O)_3Cl_6]\cdot 2CH_3CN$ (3): Complex **3** was isolated after evolution of a solution of **1** in CH_3CN in air; X-ray quality crystals were obtained by slow evaporation of the solvent CH_3CN. In an alternative method a solution of **1** in CH_3CN was heated under air at 70°C for 24 h. Crystals of **3** were obtained after an additional 24 h, when the solution was allowed to cool to room temperature. $C_{31}H_{38}Cl_6Fe_4N_6O_3$ (978.8): calcd. C 38.04, H 3.91, N 8.58; found C 37.70, H 3.87, N 8.54. FT-IR: $\tilde{\nu}$ = 1610 (s, i), 1578 (s, m), 1469 (s, i), 1456 (s, i), 854 (s, i), 818 (b, i), 790 (s, i), 352 (s, i) cm^{-1}. The three bands around 800 cm^{-1} can be attributed to Fe−O modes, by comparison with other (μ-oxo)diiron(III) complexes.[26]

[1] S. J. Lippard, J. M. Berg, *Principles of Bioinorganic Chemistry*, University Sciences Books, Mill Valley, **1994**.
[2] M. Sono, M. P. Roach, E. D. Coulter, J. H. Dawson, *Chem. Rev.* **1996**, *96*, 2841.
[3] B. J. Wallar, J. D. Lipscomb, *Chem. Rev.* **1996**, *96*, 2625.

[4] K. C. M. Costas, L. Que, K. Chen, L. Que, *Coord. Chem. Rev.* **2000**, *200−202*, 517.
[5] J. Dubois, T. J. Mizoguchi, S. J. Lippard, *Coord. Chem. Rev.* **2000**, *200−202*, 443.
[6] J.-J. Girerd, F. Banse, A. J. Simaan, *Struct. Bonding.* **2000**, *97*, 146.
[7] N. Raffard, V. Balland, J. Simaan, S. Létard, M. Nierlich, K. Miki, F. Banse, E. Anxolabéhère-Mallart, J.-J. Girerd, *C. R. Chim.* **2002**, *5*, 99.
[8] V. K. Yachandra, M. P. Klein, *Chem. Rev.* **1996**, *96*, 2927.
[9] W. Rüttinger, G. C. Dismukes, *Chem. Rev.* **1997**, *97*, 1.
[10] G. J. P. Britovsek, V. C. Gibson, B. S. Kimberley, S. Mastroianni, C. Redshaw, G. A Solan, A. J. P. White, D. J. Williams, *J. Chem. Soc., Dalton Trans.* **2001**, 1639.
[11] J. Bernal, I. M. Jensen, K. B. Jensen, C. J. Mckenzie, H. Toftlund, J-P. Tuchagues, *J. Chem. Soc., Dalton Trans.* **1995**, 3667.
[12] J. Simaan, J. Guilhem, S. Poussereau, G. Blondin, J-J. Girerd, D. Defaye, C. Philouze, J. Guilhem, L. Tchertanov, *Inorg. Chim. Acta* **2000**, *299*, 221.
[13] C. Bucher, E. Duval, J-M. Barbe, J-N. Verpeaux, C. Amatore, R. Guilard, L. Le Pape, J-M. Latour, S. Dahaoui, C. Lecomte, *Inorg. Chem.* **2001**, *40*, 5722.
[14] S. J. Brudenell, L. Spiccia, A. M. Bond, G. D. Fallon, D. C. R. Hockless, G. Lazarev, P. J. Mahon, E. R. T. Tiekink, *Inorg. Chem.* **2000**, *39*, 881.
[15] I. Romero, M-N. Collomb, A. Deronzier, A. Llobet, E. Perret, J. Pécaut, L. Lepape, J.-M. Latour, *Eur. J. Inorg. Chem.* **2001**, 69.
[16] H. Toftlund, K. S. Murray, P. R. Zwack, L. F. Taylor, O. P. Anderson, *J. Chem. Soc., Chem. Commun.* **1986**, 2673.
[17] J. L. Sessler, J. W. Sibert, V. Lynch, *Inorg. Chem.* **1990**, *29*, 4143.
[18] J. L. Sessler, J. W. Sibert, V. Lynch, J. T. Markert, C. L. Wooten, *Inorg. Chem.* **1993**, *32*, 621.
[19] N. Arulsamy, J. Glerup, D. J. Hodgson, *Inorg. Chem.* **1994**, *33*, 3043.
[20] A. K. Boudalis, N. Lalioti, G. A. Spyroulias, C. P. Raptopoulou, A. Terzis, V. Tangoulis, S. P. Perlepes, *J. Chem. Soc., Dalton Trans.* **2001**, 955.
[21] P. Gomez-Romero, G. C. Defotis, G. B. Jameson, *J. Am. Chem. Soc.* **1986**, *108*, 851.
[22] P. Gomez-Romero, E. H. Witten, W. M. Reiff, G. B. Jameson, *Inorg. Chem.* **1990**, *29*, 5211.
[23] P. Gómez-Romero, E. H. Witten, W. M. Reiff, G. Backes, J. Sanders-Loehr, G. B. Jameson, *J. Am. Chem. Soc.* **1989**, *111*, 9039.
[24] J. Wang, M. S. Mashuta, Z. Sun, J. F. Richardson, D. N. Hendrickson, R. M. Buchanan, *Inorg. Chem.* **1996**, *35*, 6642.
[25] N. Raffard-Pons Y Moll, F. Banse, K. Miki, M. Nierlich, J.-J. Girerd, *Eur. J. Inorg. Chem.* **2002**, 1941.
[26] D. M. Kurtz Jr., *Chem. Rev.* **1990**, *90*, 585.
[27] L. Yin, P. Cheng, S. P. Yan, X-Q. Fu, J. Li, D.-Z. Liao, Z.-H. Jiang, *J. Chem. Soc., Dalton Trans.* **2001**, 1398.
[28] O. Kahn, *Molecular Magnetism*, VCH Publishers, New York, Weinheim, Cambridge, **1993**.
[29] C. Philouze, G. Blondin, J.-J. Girerd, J. Guilhem, C. Pascard, D. Lexa, *J. Am. Chem. Soc.* **1994**, *116*, 8557.
[30] R. D. Dowsing, J. F. Gibson, M. Goodgame, P. J. Hayward, *J. Chem. Soc., A* **1970**, 1133.
[31] F. E. Mabbs, D. Collison, *Electron Paramagnetic Resonance of d Transition Metal Compounds*, Elsevier, Amsterdam, **1992**.
[32] P. Mialane, A. Novorojkine, G. Pratviel, L. Azéma, M. Slany, F. Godde, A. Simaan, F. Banse, T. Kargar-Grisel, G. Bouchoux, J. Sainton, O. Horner, J. Guilhem, L. Tchertanova, B. Meunier, J. J. Girerd, *Inorg. Chem.* **1999**, *38*, 1085.
[33] S. Poussereau, G. Blondin, M. Césario, J. Guilhem, G. Chottard, F. Gonnet, J.-J. Girerd, *Inorg. Chem.* **1998**, *37*, 3127.
[34] M. D. Snodin, L. Oud-Moussa, U. Wallmann, S. Lecomte, V. Bachler, E. Bill, H. Hummel, T. Weyermüller, P. Hildebrandt, K. Wiegardt, *Chem. Eur. J.* **1999**, *5*, 2554.
[35] C. A. Brown, G. J. Remar, R. L. Musselman, E. I. Solomon, *Inorg. Chem.* **1995**, *34*, 688.
[36] P. C. Junk, B. J. Mccool, B. Moubaraki, K. S. Murray, L. Spiccia, J. D. Cashion, J. W. Steed, *J. Chem. Soc., Dalton Trans.* **2002**, 1024.
[37] A. Hazell, K. B. Jensen, C. J. Mckenzie, H. Toftlund, *Inorg. Chem.* **1994**, *33*, 3127.
[38] A. Nivorozhkin, E. Anxolabéhère-Mallart, P. Mialane, R. Davydov, J. Guilhem, M. Cesario, J.-P. Audière, J.-J. Girerd, S. Styring, L. Schussler, J.-L. Seris, *Inorg. Chem.* **1997**, *36*, 846.
[39] The intensity of the oxidation wave was compared with that of a related Fe^{II} complex (ref.[7]), for which it was shown that the wave was a one-electron oxidation process.
[40] T. H. Hubin, J. M. Mccormick, N. W. Alcock, D. H. Bush, *Inorg. Chem.* **2001**, *40*, 435.
[41] N. B. V. Kappa-Ccd Software, Delft, The Netherlands, **1998**.
[42] G. M. Sheldrick, *Acta Chrystallogr., Sect. A* **1990**, 467.
[43] G. M. Sheldrick, *SHELXTL-97, Program for the refinement of crystal structures*, University of Göttingen, Germany, **1997**.
[44] G. M. Sheldrick, University of Göttingen, Germany, **1999**; distributed by Bruker AXS, Madison, Wisconsin, USA.
[45] H-R. Chang, J. K. McCuster, H. Toflund, S. R. Wilson, A. X. Trautwein, H. Winkler, D. N. Hendrickson, *J. Am. Chem. Soc.* **1990**, *112*, 6814.

Received June 18, 2003
Early View Article
Published Online February 16, 2004

